Journal of Applied Polymer Science

Acrylonitrile–Butadiene Rubber Functionalization for the Toughening Modification of Recycled Poly(ethylene terephthalate)

Mohammad Reza Raiisi-Nia,[1] Ahmad Aref-Azar,[1] Mohammad Fasihi[2]

[1]Department of Polymer Engineering and Color Technology, Amirkabir University of Technology, Tehran 15875-4413, Iran
[2]School of Chemical Engineering, Iran University of Science and Technology, Narmak, Tehran 16765-163, Iran
Corresponding author: M. Fasihi (E-mail: mfasihi@iust.ac.ir)

ABSTRACT: The incorporation of functionalized acrylonitrile–butadiene rubber (NBR) into recycled poly(ethylene terephthalate) (PET) was introduced as an effective route for modifying the properties of PET and as a new method for PET recycling as well. To achieve modified NBR, glycidyl methacrylate (GMA) was grafted onto NBR with optimized reactive mixing, in which the highest grafting degree and lowest gel content were generated. PET/NBR blends with and without GMA functionalization were produced by melt mixing, and the mechanical properties, dynamic mechanical thermal properties, and phase morphologies of the systems were determined and compared. We found that low amounts of peroxide initiator (dicumyl peroxide) and high levels of the GMA monomer in the presence of the styrene comonomer led to the maximum grafting degree and suppressed the competing rubber crosslinking and GMA homopolymerization reactions. The blend compatibility with PET determined from dynamic mechanical thermal analysis spectra and scanning electron microscopy images was greatly improved when the NBR-grafted GMA was used instead of the neat NBR in the blend recipes. As a result, the rubber phase dispersed in the PET matrix more finely, and the impact strength of the blend advanced very significantly. © 2014 Wiley Periodicals, Inc. J. Appl. Polym. Sci. **2014**, *131*, 40483.

KEYWORDS: blends; mechanical properties; morphology; polyesters; recycling

Received 23 October 2013; accepted 16 January 2014
DOI: 10.1002/app.40483

INTRODUCTION

In the packaging industry, poly(ethylene terephthalate) (PET) has experienced rapid growth since the 1970s, especially in the field of soft drink bottle applications. This is mainly due to its excellent chemical resistance and good optical and barrier properties.[1]

The recycling of PET has always been the center of much attentions because of the high production of this thermoplastic PET and its widespread use. Most methods used for recycling PET wastes are chemical recycling and mechanical recycling. The chemical recycling of PET is very attractive for its easy recycling by different ways, which give different products that can be introduced as initial components for the synthesis of many other polymers. PET can be recycled by hydrolysis, acidolysis, alkalolysis, aminolysis, alcoholysis, and glycolysis. Oligomers coming from the chemical recycling of PET waste have been applied as starting materials for the manufacturing of polyesters,[2–4] polyurethanes,[5] and so on.[6–8]

Mechanical recycling, which consists of the collection, separation, grinding, washing, extruding, and granulating of the polymer, is the most common method. Most recycled poly(ethylene terephthalate) (R-PET) flakes (>70%) are converted into fibers by mechanical recycling.[9,10] Also, many studies have been performed on the use of PET wastes in different applications, such as bottles, films, sheets, modified concrete, and industrial parts, by the application of different modifications, such as blending,[11–13] and through the creation of composites[14–16] and nanocomposites.[17–19] However, PET is a notch-sensitive thermoplastic with a low impact strength that decreases during physical aging. This has strongly lowered its potential for use in many applications. So, rubber modification has become of interest as an effective method for increasing the fracture toughness and inducing a brittle–tough transition in the fracture mode.[20–22]

Dispersed rubber particles can increase toughness by two mechanisms. They accelerate yielding by acting as stress concentrators and initiating deformation in the matrix. Second, they make voids (through cavitation or interface debonding) to alter the stress state in the surrounding matrix and allow further plastic deformation in the matrix to develop.[20] The ultimate mechanical properties depend impressively on the blend characteristics and its constituting components. It is generally known that the blend morphology plays a very important role in the

Table I. Characteristics of the Materials Used for the Blending of PET and NBR

Material	Company	Property	
Virgin poly(ethylene terephthalate)	V-PET	Tex Pet (Korea)	T_m = 246°C, IV = 0.8
Recycled poly(ethylene terephthalate) (flake)	R-PET	—	T_m = 250.74°C
NBR	NBR34	KNB 35L (Korea)	ACN content = 34%, MV = 41
	NBR50	Krynac 5075 (Germany)	
	ACN content = 50%, MV = 75		
	NBR blend[a]	—	—

T_m, melting temperature; IV, intrinsic viscosity; MV, Mooney viscosity.
[a] We prepared this mixture by mixing equal amounts of NBR34 and NBR50.

toughening efficiency.[20,23,24] The addition of elastomers results in an improved overall toughness if the rubber phase is finely dispersed on the submicrometer level in the polymer matrix. The most important factors that greatly influence the phase morphology are the rubber type and concentration, mixing conditions, interfacial effects, and component molecular weights.[25,26]

Reactive compatibilization is known as an effective method for improving the interfacial adhesion and morphology control in various incompatible blends. Some types of elastomers and functional groups, such as ethylene–propylene rubber grafted with maleic anhydride and ethylene–propylene–diene rubber grafted with maleic anhydride, have been used in PET blends.[27–29] Furthermore, effective compatibilization between PET and ethylene–propylene rubber elastomer, high-density polyethylene, and styrene-ethylene/butylene-styrene (SEBS) has been observed in the presence of glycidyl methacrylate (GMA) functional groups in separate studies.[30–32] In addition to these, in a comparative compatibilization study of PET/polypropylene (PP) blends, GMA-functionalized PP was found to be more effective than maleated PP.[33]

Considering the low impact strength of PET, its deterioration during physical aging, and the effectiveness of the GMA function on compatibilization, as demonstrated in the literature, our strategy to overcome the low impact strength of PET was to produce PET-based blends through the use of GMA-functionalized acrylonitrile–butadiene rubber (NBR). So, the aim of this study was to produce PET/NBR-*g*-GMA blends and to check whether or not the mechanical performance could be upgraded by rubber modification. This method was considered as a recycling option for waste PET bottles.

EXPERIMENTAL

Materials

Commercial bottle-grade PET (Tex Pet, Korea) and waste PET from a local market were used as the base materials. The applied rubber materials were NBR34 (acrylonitrile content = 34 ± 1%, Kumho Petrochemical, Korea) and NBR50 (acrylonitrile content = 50 ± 1%, Bayer AG, Germany). Other chemicals used in the grafting process were GMA, dicumyl peroxide (DCP), and styrene comonomer; these were all purchased from Merck (Germany). Commercial methyl ethyl ketone (MEK), methanol, and acetone prepared by a local company were used as solvents. The applied materials and with their basic characterizations are listed in Table I.

Equipment

An internal batch mixer (Brabender W50, PL2200) with a chamber capacity of 60 mL was used for grafting of the NBR functionalization and for preparing the PET/NBR blends. The IR spectrometry analysis was performed on a BOMEM (Canada) Fourier transform infrared (FTIR) apparatus. Scanning electron microscopy (Cambridge S360) was used to study the morphologies of the samples. The Izod (notched) impact strengths of the specimens were determined according to ASTM D 256 on a U-F impact tester (Ueshima Manufacturing Co., Japan). Tensile tests were performed on a Galdabini tester (Sun 2500, Italy) according to ASTM D 638 with a crosshead speed of 50 mm/min. Dynamic mechanical thermal analysis measurements were carried out on a dynamic mechanical thermal analysis (PL-DMTA model) in bending mode with a frequency of 1 Hz in the temperature range −50 to 140°C at a heating speed of 5°C/min.

NBR Functionalization Procedure

Eight formulations designed to obtain optimal conditions for the grafting process are listed in Table II. For the grafting process, NBR first was dried at 80°C for 6 h and was then fed into the internal mixer at 175°C. After that, styrene comonomer (for formulations G4 and G8), GMA, and DCP were added at 1-min intervals, respectively. The mixing continued for 5 min. After the reaction was finished, the samples were discharged from the mixing chamber and cooled to room temperature.

Table II. Formulations Used for the Grafting Process

Sample	DCP (phr)	GMA (phr)	Styrene (phr)
G1	0.6	6	0
G2	0.3	6	0
G3	0.1	6	0
G4	0.3	6	6
G5	0.1	8	0
G6	0.1	10	0
G7	0.05	10	0
G8	0.05	10	10

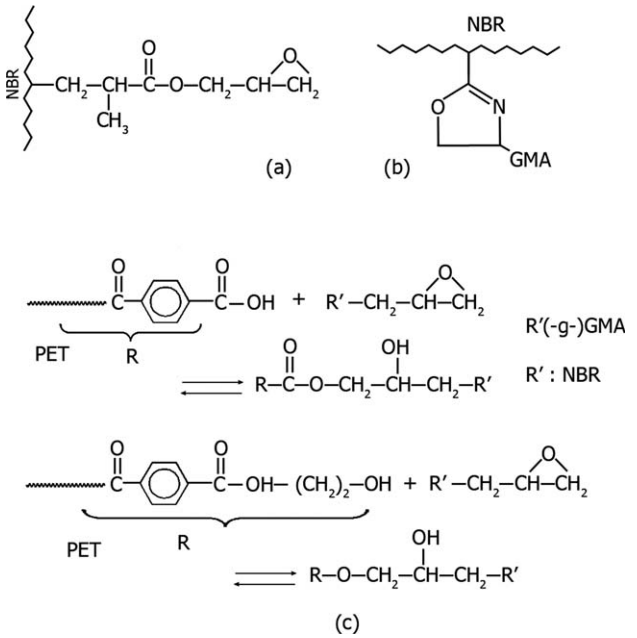

Figure 1. Grafting of GMA onto NBR: (a) epoxy end group, (b) oxazoline structure, and (c) reaction of the epoxide groups with the end groups of PET.

During the grafting procedure, three different reactions occurred: the grafting of GMA on to NBR, GMA homopolymerization or copolymerization by the commoner, and the cross-linking of the rubber molecules (gel). The amount of grafted and homopolymerized GMA was determined by the application of the purification method. The gel content was determined according to ASTM D 3616, in which 0.4 g of reacted NBR was dissolved in MEK and stirred at 85°C for 24 h. Then, the solution was filtered. The remaining precipitate was measured as a gel. For identification of the polymerized glycidyl methacrylate (Poly-GMA), 3 g of reacted NBR was completely dissolved in MEK. Half of the produced solution was precipitated in acetone, and the remaining half was precipitated in methanol. Because Poly-GMA could be dissolved in acetone but not in methanol, the weight percentage of Poly-GMA could be calculated by the deduction of two precipitates' weights.

The grafting of GMA on NBR could proceed by two separate routes: first, the reaction of GMA double bonds with NBR macroradicals and, second, the reaction of GMA epoxide groups with the cyanide group on NBR to form an oxazoline structure. The products of both reactions were capable of reacting with the end groups of the PET molecules. These reactions are shown in Figure 1.

The GMA content of the functionalized NBR was determined by FTIR spectroscopy. The quantity of the functional units was determined by the integration of the appropriate signals.[34] The characteristic signals in the spectra (Figure 2) were found at 1720 cm^{-1} for the carbonyl stretching vibration of GMA and at about 1450 cm^{-1} for the CH_2 bending band. Because of the reaction between the GMA epoxide groups and CN groups of NBR molecules and the formation of oxazoline groups, the signals at about 2237 cm^{-1}, which belonged to the CN groups of NBR, could not be used effectively for the evaluation of the grafting percentage. According to the following equation, the relative percentage of grafted GMA was calculated:

$$\left(\frac{A_{CH}}{A_{CO}}\right)_{GMA}=0.42$$
$$\frac{W_{GMA}}{W_{NBR}}=\frac{A_{CO}}{(A_{CH})_{NBR}}=\frac{A_{CO}}{A_{CH}-(A_{CH})_{GMA}}=\frac{A_{CO}}{A_{CH}-0.42A_{CO}} \quad (1)$$

where W is the weight percent and A is the FTIR peak area.

PET/NBR Blend Preparation

To study the effects of variable factors such as rubber concentration, rubber type, and screw speed on the mechanical properties of the blends, an experimental design from the Taguchi method was adopted. By applying this technique, we reduced the number of experimental runs significantly. Minitab Software was used for the planning experiments and analysis of the results on basis of the Taguchi method. An L9 orthogonal array was used for three factors at three levels and is shown in Table III. Furthermore, to study the effect of NBR-*g*-GMA and this kind of PET on the properties of the blends, five other formulations were designed and are listed in Table IV.

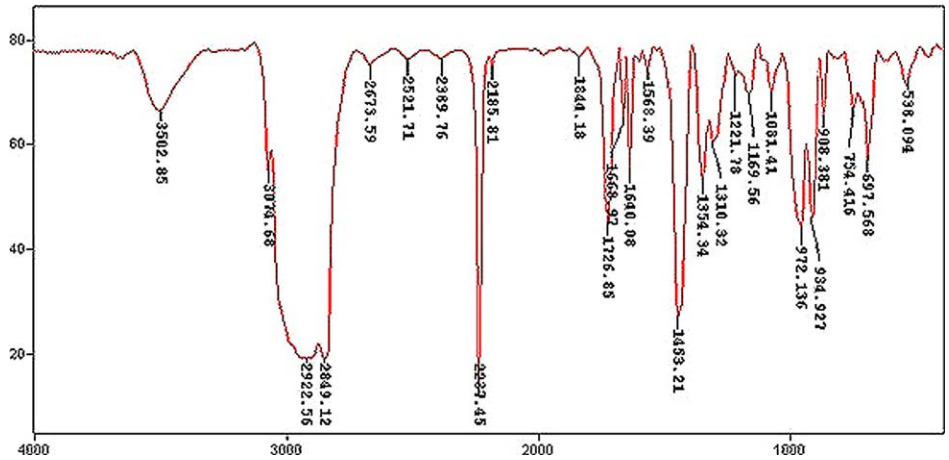

Figure 2. FTIR curve of G5 that shows oxazoline, epoxide, and CN groups on the grafted NBR. [Color figure can be viewed in the online issue, which is available at wileyonlinelibrary.com.]

Table III. Samples Prepared According to the Taguchi Experimental Design

Sample	NBR (phr)	NBR type	Screw speed (rpm)	PET type
B1	10	NBR34	35	R-PET
B2	20	Blend[a]	35	R-PET
B3	30	NBR50	35	R-PET
B4	20	NBR34	50	R-PET
B5	30	Blend[a]	50	R-PET
B6	10	NBR50	50	R-PET
B7	30	NBR34	65	R-PET
B8	10	Blend[a]	65	R-PET
B9	20	NBR50	65	R-PET

[a] We prepared this mixture by mixing equal amounts of NBR34 and NBR50.

RESULTS AND DISCUSSION

GMA Grafting onto NBR

The GMA grafting degree, gel content, and formed percentage of Poly-GMA for formulations G1–G8 were measured according to the mentioned procedures, and the results are reported in Table V.

For samples G3, G2, and G1, an increase in the DCP concentration resulted in an increase in the grafting degree and a rise in the gel content. This increase in grafting was as a result of the higher concentration of free radicals with regard to the higher DCP content, which created more NBR macroradicals. The gel content also increased because of the crosslinking of rubber chains and also the formation of poly-GMA. So, high grafting degrees were accompanied by increasing crosslinking reactions.

On the other hand, when the GMA concentration was increased in formulations G3, G5, and G6, the grafting degree increased. This was in line with previous studies.[30,35,36] This was indeed due to the higher possibility of GMA grafting onto the formed macroradicals as a result of the higher GMA monomer concentration in the system.

With a higher GMA concentration, the lower gel content led to fewer possible crosslinking reactions; however, it increased the homopolymerization of GMA, which caused the GMA grafting degree to decrease.

Table IV. Formulation Designed to Study the Effects of the Compatibilizer and the Type of PET

Sample	NBR (phr)	ACN (%)	Screw speed (rpm)	PET type
B10	20 (NBR34)	34	50	V-PET
B11	10 (NBR-*g*-GMA)	34	50	R-PET
B12	20 (NBR-*g*-GMA)	34	50	R-PET
B13	30 (NBR-*g*-GMA)	34	50	R-PET
B14	20 (NBR50)	34	50	R-PET

Table V. GMA Grafting Degree, Gel Content, and Poly-GMA Percentage

Sample	Relative grafting degree	Gel content (%)	Poly-GMA (%)
G1	0.85	88	2.8
G2	0.70	68	2.5
G3	0.56	52	2.1
G4	1.13	60	1.7
G5	0.63	46	2.2
G6	0.72	40	2.4
G7	0.68	27	2.2
G8	1.26	14	0.8

As reported in the literature, the use of a comonomer with an approximately equal molar ratio accompanying GMA led to a decrease in undesirable side reactions and an increase the efficiency of the grafting reaction.[30,35,37,38]

A comparison of the results of the gel and grafting contents of samples G2 and G4 (Table V) revealed that with the addition of the styrene comonomer to the system, the GMA grafting degree increased, and the gel content decreased. This attractive effect occurred because the styrene monomer was more active than the GMA molecule. Therefore, it reacted readily with macroradicals, and because the formed radical was more stable for the benzene ring resonance, the possibility of GMA grafting on to NBR molecules increased. On the other hand, styrene reacted faster with NBR macroradicals, and thus, the reaction of macroradicals with each other decreased and lowered the gel content. Because samples G1–G6 contained high levels of gel content, low amounts of DCP initiator were applied to decrease gel formation in samples G7 and G8. A comparison between the reactions of samples G7 and G8 (Table V) showed that with the addition of the styrene comonomer in equal molar ratios with GMA and a decrease in the amount of initiator to 0.05 phr, the highest grafting degree and the lowest amount of nondesirable side reactions were obtained.

Figure 3 illustrates the torque–time curves for samples G1, G3, G7, and G8. From about the middle of mixing, the torque increased as a result of the occurrence of competitive reactions (grafting, crosslinking, and homopolymerization). The higher concentration of DCP in sample G1 caused the formation of higher amounts of free radicals, including macroradicals. Thus, the crosslinking and branching of NBR molecules progressed more, and the viscosity of the melt increased suddenly. Then, some parts of the formed networks were broken down by the remaining radicals, and the torque decreased slightly. In the final stage of mixing, because radicals were consumed, the torque curve approached a constant value of almost 36 N m. Although the torque–time curve for sample G3, which had a lower amount of DCP, revealed that the grafting and crosslinking reactions proceeded on a limited basis, the enhancement in the viscosity was much lower than in the previous case, and the torque curve became steady after a while to a value of 32 N m.

As noticed before, the use of styrene as a comonomer decreased the crosslinking side reactions and increased the degree of

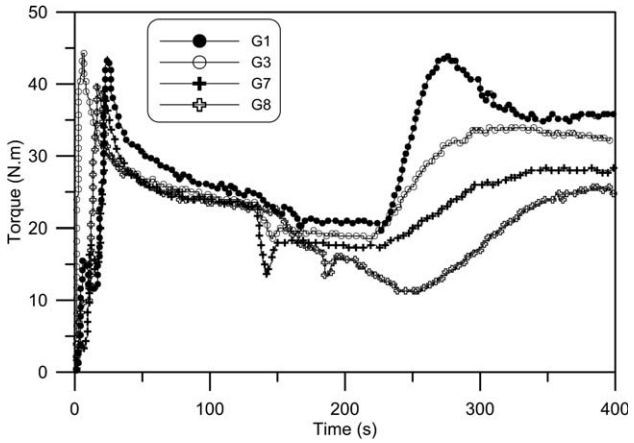

Figure 3. Torque–time curves for G1, G3, G7, and G8.

grafting. A comparison between the torque–time curves for samples G7 and G8 (Figure 3) showed that in the presence of styrene comonomer (sample G8), the final torque at the end of mixing was lower (ca. 21 N m). This was attributed to the lower gel formation during the grafting reaction.

By comparing the results of different formulations used in the grafting procedure, we found that sample G8 had the highest degree of grafting and the lowest extent of side reactions. Therefore, this sample was used as the compatibilized rubber in the formulations of the PET/NBR-*g*-GMA blends.

Tensile Properties of the PET/NBR Blends

First, an experimental design based on the Taguchi approach was applied to optimize the concentration of materials and processing parameters for the blend of PET and neat NBR. For this purpose, the tensile and impact strengths of nine runs designed by the Taguchi approach were compared with each other, and optimum conditions were obtained. Then, those conditions were selected to prepare PET/NBR-*g*-GMA blends, and their properties were compared with those of the noncompatibilized blends.

The tensile test results are shown in Figure 4. Statistical analysis indicated that the NBR type had a significant effect on the tensile strength. The middle level of NBR type (the NBR blend) showed the lowest tensile strength; this could be attributed to possible poor dispersion and poor compatibility between the phases when two kinds of rubber were used in the formulations simultaneously. The samples with 34 and 50% acrylonitrile (ACN) had close tensile strengths. When the NBR content was increased, the tensile strength decreased to a nonstrong interaction between the dispersed rubber and the PET matrix. It was also shown that the screw speed had a minor effect on the tensile strength, and the blend with the middle level speed (50 rpm) showed slightly better properties.

The elongation at break values of the samples represented almost similar trends except that the elongation at break versus the NBR content showed a maximum at 20 phr NBR. The decrease in the elongation at break at a high level of NBR (30 phr) might have been due to poor dispersion and the coalescence of rubber particles in blends with high volume fractions

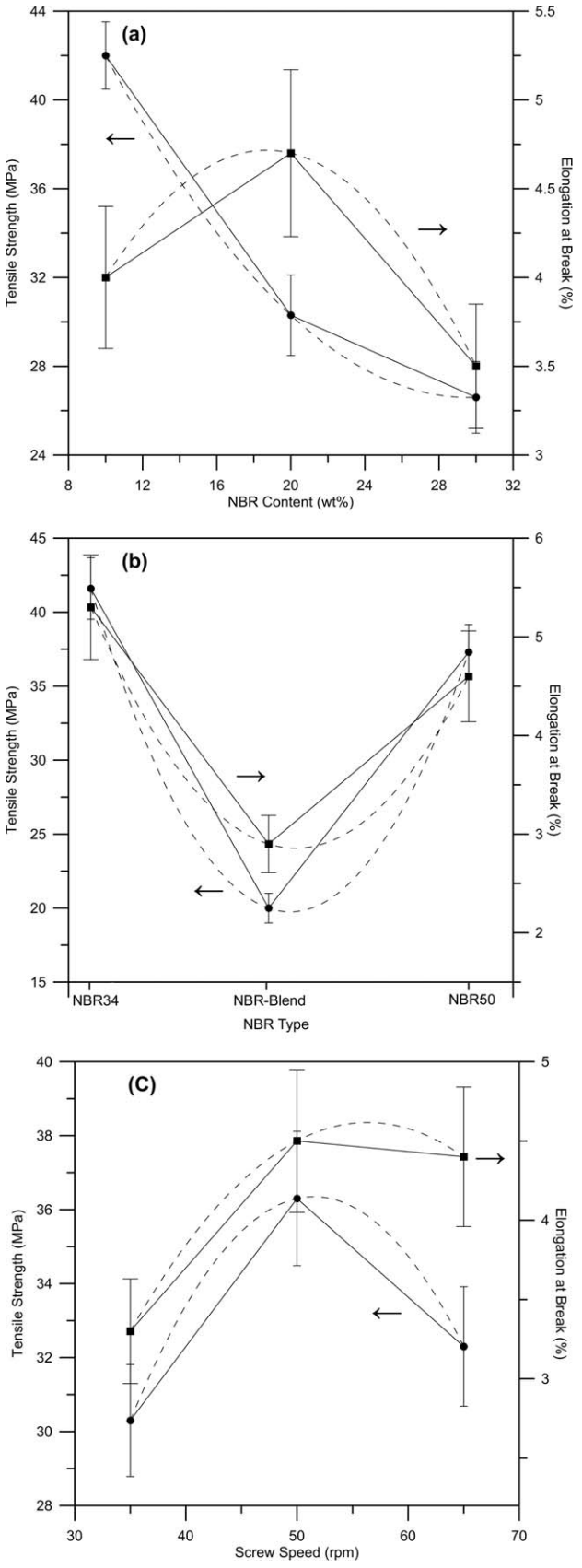

Figure 4. Effect of the various factors on the tensile strength and elongation at break.

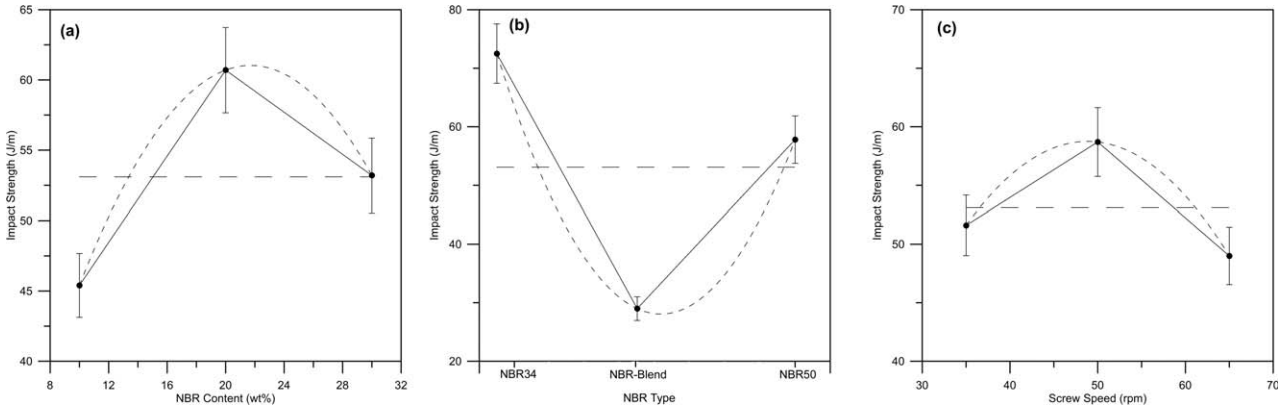

Figure 5. Effect of the different factors on the impact strength.

of rubber. When the ACN percentage was increased, the strength (and stiffness) of the rubbery phase in the blends increased, but strain hardening of the rubber phase decreased. This was believed to be the reason for the higher tensile strength and elongation at break observed for blends prepared with NBR34 compared to the blends prepared with NBR50. For blends containing a mixture of NBR34 and NBR50, because of the poor compatibility between phases, the elongation at break decreased considerably as well. The screw speed also had a minor effect on the elongation at break. Under optimum conditions, the elongation at break of the blend presented 69 and 111% higher values than those of virgin poly(ethylene terephthalte) (V-PET; 3.5%) and R-PET (2.8%), respectively.

Impact Strength

The notched impact strengths of the samples are presented in Figure 5. As shown, the NBR type was the most important parameter that affected the impact strength. When the ACN percentage was increased from 34 to 50%, the impact strength first decreased dramatically by 55% and then increased by twofold to about 58 J/m. The lowest impact strength at the middle percentage of ACN (in the NBR blend) was perceived be due to the poor dispersion of rubber when the mixture with two kinds of rubber, NBR34 and NBR50, was used to mix with the PET matrix. The rubber content and screw speed had slight effects on the impact strength, but the compounds with middle levels (20-phr NBR content and 50-rpm screw speed) showed better impact strengths. The best results for the impact strength were obtained with NBR34 at 20-phr NBR and a screw speed of 50 rpm. Under these conditions, the values of impact strength were 3.5 and 2 times greater than that of R-PET (19.6 J/m) and V-PET (34.6 J/m), respectively.

PET/NBR-*g*-GMA Blends

By optimizing the conditions based on the mechanical results of PET/NBR, we designed five extra formulations for the comparative study of the effect of the use of modified NBR instead of natural NBR; these are listed in Table IV. The goal of this part was a comparative study of the mechanical properties and morphology of the blends and to highlight the role of NBR-*g*-GMA.

Dynamic Mechanical Analysis (DMA) Studies of the Compatibilized Blends

DMA was applied to study the miscibility in the blends and also to measure the glass-transition temperatures (T_g's) of the polymers and blends. The damping factor peak (tan δ) corresponded to the maximum heat dissipation per unit deformation. T_g was selected as the peak position of tan δ when it was plotted as a function of the temperature. The T_g values obtained by DMA for the pure polymers were 100, 98, 11.1, and -12.4°C for V-PET, R-PET, NBR50, and NBR34, respectively. The variation of tan δ with the temperature of samples B2, B4, and B12 are given in Figure 6. For sample B2, in which two kinds of NBR were used equally, two T_g's were present at low temperatures close to the T_g's of two rubbers and one narrow peak was present at a high temperature and was related to the T_g of PET. This indicated that these two rubber grades had poor compatibility, and hence, lower mechanical properties were observed in these blends.

Samples B4 and B12 showed the presence of two peaks corresponding to the T_g's of NBR34 and PET. The upper peak of both samples, especially B12, was broadened in comparison with those of neat PET and B2. The broadening of the peaks was an indication of compatibilization. The general broadening of the tan δ peaks was associated with increased molecular mixing.[39] As the compatibility increased, the interpenetration of the components increased. There was also an appreciable shift in the T_g toward the average value in B12. The difference between the low and high tan δ peaks of sample B4 was 104.7°C and

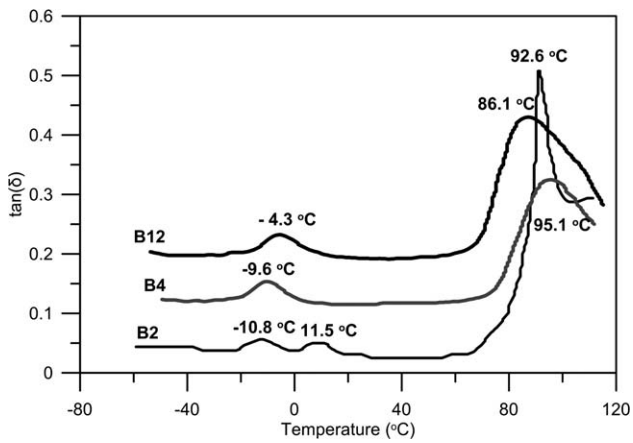

Figure 6. Tan δ curves as a function of the temperature for samples B2, B4, and B12.

Table VI. Tensile Results for Different Samples

Sample	Tensile strength (MPa)	Elongation at break (%)
B10	43	6.2
B11	47	5.3
B12	44	8.1
B13	32	8.3
B14	42	3.8
V-PET	60	3.5
R-PET	54	2.8

Table VII. Impact Strength Results for Different Formulations

Sample	Impact strength (J/m)
B10	93.5
B11	80.4
B12	110.6
B13	117.3
B14	60.8
V-PET	34.6
R-PET	19.6

was lowered to 90.4°C for B12. This emphasized that a significant miscibility increase occurred for the compatibilized blend.

Tensile Tests of the Compatibilized Blends

The tensile strength and elongation at break of the compatibilized blends are presented in Table VI and Figure 7. As compared to pure PET, the presence of elastomer dispersed in the PET matrix decreased the tensile strength. The pure PET just showed an elastic deformation, whereas the compatibilized blend demonstrated both elastic and plastic deformations.

A comparison between B14 and B12 revealed that the use of NBR-*g*-GMA in the blend resulted in two increases in the elongation at break and resulted in stronger adhesion between the two phases. When the rubber content in the blends containing NBR-*g*-GMA (samples B11, B12, and B13) was increased, the elongation at break increased. This was attributed to the finer dispersed rubber and lower coalescence of the rubber particles in the presence of the modified rubber. The tensile strength, with increasing modified rubber content in these blends, still decreased because of the lower tensile strength of the rubber phase in comparison with those of PET.

Impact Tests

The results of the impact strength of the compatibilized blends are listed in Table VII. With NBR-*g*-GMA instead of pure NBR in the blend, a further increase in the value of the impact strength was observed. This was perceived as a result of the reactions taking place in the interface and bond formation between the epoxide and oxazoline groups of the grafted rubber with the hydroxyl and carboxyl end groups of PET, which led to stronger adhesion of the two phases. The impact strength of the compatibilized blends with different NBR-*g*-GMA contents in B11, B12, and B13 showed surprisingly up to 32, 55, and 80% improvements, respectively, in comparison with the noncompatibilized blends with the same rubber contents. The impact strength of B12 was wonderfully 3 and 5.5 times greater than those of V-PET and R-PET, respectively. This result confirms the fine dispersion of the rubber phase in the blend and adequate interfacial adhesion between the modified NBR and PET phases.

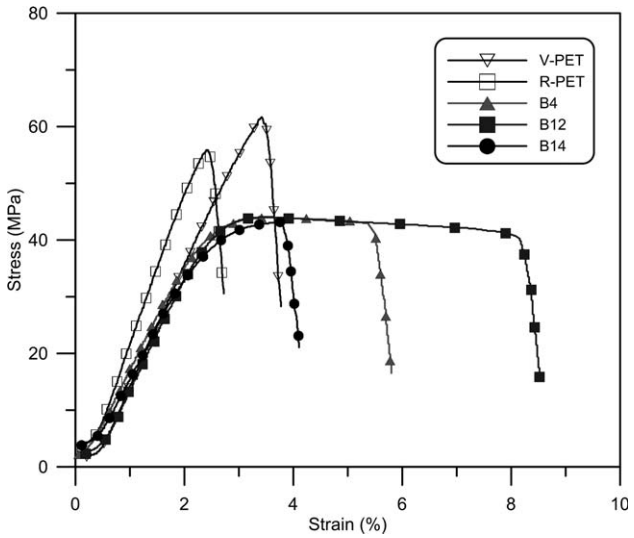

Figure 7. Stress–strain curve of different samples.

Morphology of the Blends

Figure 8 shows micrographs for samples B4, B6, and B12. The rubber phase dispersed in the size range from 0.3 to 5 μm. The average size of the rubber particles was measured with ImageJ software. A comparison between Figures 8(a) and 8(b) showed that in the sample B6, the particles (average = 2 μm, range = 1–4.5 μm) were smaller and were distributed more evenly than in B4 (average = 3.5 μm, range = 1.9–6 μm). In the literature, the solubility parameter of PET was reported to be equal to 21.5 $(j/cm^3)^{0.5}$, and that of NBR (with 30–50% ACN) was reported to be in the range 19.2–21.3 $(j/cm^3)^{0.5}$, which increased with increasing acrylonitrile percentage.[40] So, theoretically, NBR50 should have been more compatible with PET than NBR34. Because B4 contained NBR34 and B6 was made of NBR50, we concluded that the closer solubility parameter or lower interfacial tension in B6 led to finer rubber particles in the B6 sample. The size of the rubber phase in the compatibilized blend was even smaller than in B6. A comparison between B6 and B12, in which NBR-*g*-GMA was used, showed that in sample B12, the particle sizes (average = 1.2 μm, range = 0.3–2.8 μm) were lowered, and a better dispersion was generated as a result of the better compatibility between PET and NBR-*g*-GMA.

CONCLUSIONS

NBR-*g*-GMA was successfully prepared by melt reactive mixing. The quality of the grafting process was influenced by the GMA and DCP concentrations and the presence of the styrene comonomer. An experimental design based on the Taguchi approach was used to study and optimize the properties of the PET/NBR blend. Grafted NBR was used to prepare a compatibilized PET/

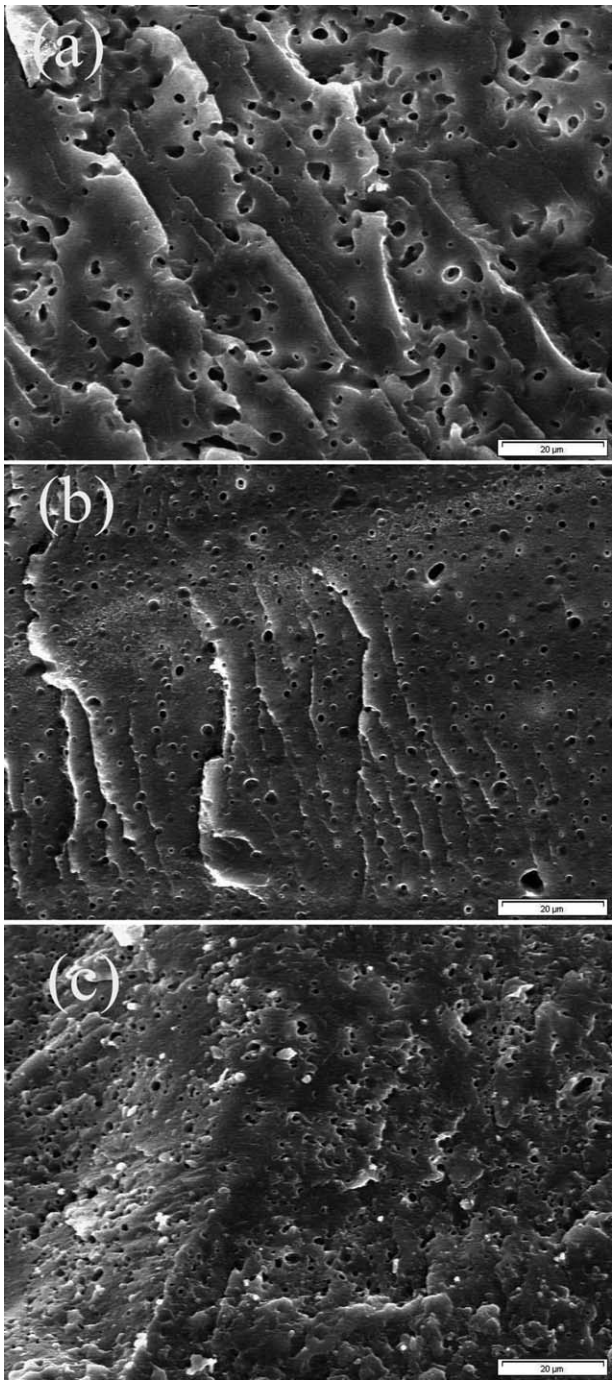

Figure 8. Scanning electron microscopy illustration for formulations (a) B4, (b) B6, and (c) B12.

NBR-*g*-GMA blend, and its properties were compared with the noncompatibilized one. The results of DMA show a lower difference in the T_g peaks in the compatibilized blend; this indicated an improved interaction between the two components in the PET/NBR-*g*-GMA system. In view of the blend morphology, the particle sizes of NBR-*g*-GMA in the PET matrix were finer than those of NBR, and the PET/NBR-*g*-GMA blends showed more homogeneous dispersions. Although the blending of PET with the NBR elastomer caused an increase in the impact strength of PET, the use of NBR-*g*-GMA in the blends instead of pure NBR improved the impact strength of the blend to much higher values. PET/NBR-*g*-GMA with 20-phr modified rubber surprisingly showed 300, 550, and 80% improvements in the impact strength in comparison with V-PET, R-PET, and noncompatibilized PET/NBR, respectively, with the same rubber content. So, this way of blending could be a good method for the recycling of waste PET bottles to widen its applications and consumption.

REFERENCES

1. Welle, F. *Resour. Conserv. Recycling* **2011**, *55*, 865.
2. Dullius, J.; Ruecker, C.; Oliveira, V. o.; Ligabue, R.; Einloft, S. *Prog. Org. Coat.* **2006**, *57*, 123.
3. Nikles, D. E.; Farahat, M. S. *Macromol. Mater. Eng.* **2005**, *290*, 13.
4. Atta, A. M. *Polym. Int.* **2007**, *56*, 984.
5. Lusinchi, J. M.; Pietrasanta, Y.; Robin, J. J.; Boutevin, B. *J. Appl. Polym. Sci.* **1998**, *69*, 657.
6. Pingale, N. D.; Shukla, S. R. *Eur. Polym. J.* **2008**, *44*, 4151.
7. Viana, M. E.; Riul, A.; Carvalho, G. M.; Rubira, A. F.; Muniz, E. C. *Chem. Eng. J.* **2011**, *173*, 210.
8. Lopez-Fonseca, R.; Gonzalez-Marcos, M. P.; Gonzalez-Velasco, J. R.; Gutierrez-Ortiz, J. I. *J. Chem. Technol. Biotechnol.* **2009**, *84*, 92.
9. Shena, L.; Worrell, E.; Patel, M. K. *Resour. Conserv. Recycling* **2010**, *55*, 34.
10. Shukla, S. R.; Harad, A. M.; Jawale, L. S. *Waste Manage.* **2008**, *28*, 51.
11. Akovali, G.; Karababa, E. *J. Appl. Polym. Sci.* **1998**, *68*, 765.
12. Kayaisang, S.; Amornsakchai, T.; Saikrasun, S. *Polym. Adv. Technol.* **2009**, *20*, 1136.
13. Lopes, C. M. A.; Goncalves, M. C.; Felisberti, M. I. *J. Appl. Polym. Sci.* **2007**, *106*, 2524.
14. Albano, C.; Camacho, N.; Hernandez, M.; Matheus, A.; Gutierrez, A. *Macromol. Symp.* **2009**, *286*, 195.
15. Ronkay, F.; Czigany, T. *Polym. Adv. Technol.* **2006**, *17*, 830.
16. Mondadori, N. M. L.; Nunes, R. C. R.; Zattera, A. J.; Oliveira, R. V. B.; Canto, L. B. *J. Appl. Polym. Sci.* **2008**, *109*, 3266.
17. Bizarria, M. T. M.; Giraldi, A. L. F. M.; Carvalho, C. M. d.; Velasco, J. I.; Vila, M. A. d. A.; Mei, L. H. I. *J. Appl. Polym. Sci.* **2007**, *104*, 1839.
18. Kráčalík, M.; Studenovský, M.; Mikešová, J.; Sikora, A. N.; Thomann, R.; Friedrich, C.; Fortelný, I.; Imoník, J. S. *J. Appl. Polym. Sci.* **2007**, *106*, 926.
19. Kráčalík, M.; Studenovský, M.; Mikešová, J.; Kovářová, J.; Sikora, A. N.; Thomann, R.; Friedrich, C. *J. Appl. Polym. Sci.* **2007**, *106*, 2092.
20. Paul, D. R.; Bucknall, C. B. Polymer Blends, Vol. 2: Performance; Wiley: New York, **2000**.
21. Araki, T.; Tran-Cong-Miyata, Q.; Shibayama, M., Structure and Properties of Multiphase Polymeric Materials; CRC: New York, **1998**.

22. Collyer, A. A. Rubber Toughened Engineering Plastics; Chapman & Hall: Cambridge, MA, **1994**.
23. Kanai, H.; Sullivan, V.; Auerbach, A. *J. Appl. Polym. Sci.* **1994**, *53*, 527.
24. Borggreve, R. J. M.; Gaymans, R. J.; Schuijer, J.; Housz, J. F. I. *Polymer* **1987**, *28*, 1489.
25. Oshinski, A. J.; Keskkula, H.; Paul, D. R. *Polymer* **1992**, *33*, 284.
26. Dompas, D.; Groeninckx, G.; Isogawa, M.; Hasegawa, T.; Kadokura, M. *Polymer* **1994**, *35*, 4760.
27. Wu, S. *Polymer* **1985**, *26*, 1855.
28. Penco, M.; Pastorino, M. A.; Occhiello, E.; Garbassi, F.; Braglia, R.; Giannotta, G. *J. Appl. Polym. Sci.* **1995**, *57*, 329.
29. Cecere, A.; Greco, R.; Ragosta, G.; Scarinzi, G.; Taglialatela, A. *Polymer* **1990**, *31*, 1239.
30. Al-Malaika, S.; Kong, W. *Polymer* **2005**, *46*, 209.
31. Pracella, M.; Rolla, L.; Chionna, D.; Galeski, A. *Macromol. Chem. Phys.* **2002**, *203*, 1473.
32. Pracella, M.; Chionna, D. *Macromol. Symp.* **2004**, *218*, 173.
33. Asgari, M.; Masoomi, M. *Compos. B* **2012**, *43*, 1164.
34. Papke, N.; Karger-Kocsis, J. *J. Appl. Polym. Sci.* **1999**, *74*, 2616.
35. Al-Malaika, S.; Kong, W. *J. Appl. Polym. Sci.* **2001**, *79*, 1401.
36. Hu, G.-H.; Cartier, H. *J. Appl. Polym. Sci.* **1999**, *71*, 125.
37. Loyens, W.; Groeninckx, G. *Macromol. Chem. Phys.* **2002**, *203*, 1702.
38. Pazzagli, F.; Pracella, M. *Macromol. Symp.* **2000**, *149*, 225.
39. Komalan, C.; George, K. E.; Kumar, P. A. S.; Varughese, K. T.; Thomas, S. *eXPRESS Polym. Lett.* **2007**, *1*, 641.
40. Brandrup, J.; Immergut, E. H.; Grulke, E. A., Polymer Handbook; Wiley: New York, **1999**.